

На прикладі осьового вентилятора ВО 06-300-4 визначається і порівнюється точність динамічного балансування обертових частин в зборі (крільчатки) коригуванням мас і пасивними автобалансирами. Крільчатка балансується в двох площинах корекції – з боку обтічника і з боку хвостовика електродвигуна.

Встановлено, що до балансування величини середніх квадратичних значень (СКЗ) віброшвидкостей на кожусі вентилятора з запасом відповідають класу точності балансування: обертові – G2,5; повні – G6,3. Основним джерелом вібрацій є динамічна залишкова незрівноваженість крільчатки. Основна складова віброшвидкостей – обертова (частота 25 Гц), тобто може бути зменшена балансуванням. Необертові складові відбуваються з субгармонійними частотами 25/2 і 25/3 Гц і на порядок менші.

При балансуванні крільчатки коригуванням мас початкові незрівноваженості з боку крільчатки і хвостовика, відповідно, 81,4 та 115,2 г·мм, а залишкові – 7,4 та 7,2 г·мм. Величини СКЗ віброшвидкостей можна зменшити на кожусі вентилятора до величин, що відповідають класу точності балансування (з запасом): обертові – G0,4; повні – G2,5. Основний внесок в залишкові вібрації дають необертові складові, що відбуваються з субгармонійними частотами.

При динамічному балансуванні крільчатки двома кульовими автобалансирами, за наявності будь-яких незрівноваженостей (в двох площинах корекції), що можуть збалансувати автобалансири, СКЗ віброшвидкостей на кожусі вентилятора відповідають класу точності балансування: обертові – G1; повні – G2,5. Кульові автобалансири реагують на незрівноваженості, що складають не менше 3% від їх балансувальної ємності. Залишкові незрівноваженості не стабільні, але не перевищують з боку крільчатки і хвостовика, відповідно, 22,2 г·мм і 21,6 г·мм.

Результати досліджень застосовні для осьових вентиляторів низького тиску, зокрема, ВО 06-300/ВО-12-300; VOG/VO-15-320; VO 2,3-130/VO 46-130. Дозволяють приймати рішення про доцільність балансування вентиляторів пасивними автобалансирами

**Ключові слова:** осьовий вентилятор низького тиску, балансування, кульовий автобалансир, автоматичне балансування, балансування коригуванням мас, віброшвидкість

UDC 62-752+62-755 : 621.634

DOI: 10.15587/1729-4061.2019.184546

# EXPERIMENTAL STUDY OF THE ACCURACY OF BALANCING AN AXIAL FAN BY ADJUSTING THE MASSES AND BY PASSIVE AUTO-BALANCERS

**I. Filimonikhina**

PhD, Associate Professor

Department of Mathematics and Physics\*\*

E-mail: fii@online.ua

**Yu. Nevdakha**

PhD, Associate Professor\*

E-mail: kntudmpmnjua@ukr.net

**L. Olijnichenko**

PhD, Engineer

Department of Materials Science and Foundry\*\*

E-mail: loga\_lubov@ukr.net

**V. Pukalov**

PhD, Associate Professor\*

E-mail: pukalovvictor@gmail.com

**H. Chornohlazova**

PhD, Senior Lecturer

Department of Aviation Engineering

Flight Academy of National Aviation University

Dobrovol'skoho str., 1, Kropivnitsky, Ukraine, 25005

E-mail: ch\_hanna@ukr.net

\*Department of Machine Parts

and Applied Mechanics\*\*

\*\*Central Ukrainian National Technical University

Universytetskyi ave., 8, Kropyvnytskyi, Ukraine, 25006

Received date 05.09.2019

Accepted date 18.11.2019

Published date 10.12.2019

Copyright © 2019, I. Filimonikhina, Yu. Nevdakha, L. Olijnichenko, V. Pukalov, H. Chornohlazova

This is an open access article under the CC BY license

(<http://creativecommons.org/licenses/by/4.0>)

## 1. Introduction

Low-pressure axial fans have been widely used in various industries [1]. These fans include axial fans of the series VO 06-300/VO-12-300; VOG/VO-15-320; VO 2,3-130/VO 46-130, produced in Ukraine [2].

There is a general issue related to reducing the noise and vibrations of axial fans. The main source of noise and vibration is the mass and aerodynamic imbalances of impellers [3–7], the design of impellers [8–12].

In axial fans, an analogy between the mass and aerodynamic imbalances is observed [6, 7, 13–16]. Therefore,

they can be balanced at the same time, for example, by correction mass (in the manufacture of a fan). Studies into the aerodynamic imbalance of low-pressure axial fans revealed that it was predominantly related to momentum [15, 16]. In addition, an impeller could be mounted onto the shaft with a skew, which would introduce a momentum component to the mass imbalance. Therefore, the impeller should be balanced dynamically, in two planes of correction.

During axial fan operation, both imbalances can change due to wear and deformation of the blades, due to dirt sticking to the blades, etc. Therefore, the impellers of axial fans should be constantly additionally balanced during operation

by passive auto-balancers. Passive auto-balancers, in particular of the ball type, have been applied for balancing high frequency rotors during operation. In the ball auto-balancers, under certain conditions, the balls themselves come to the position wherein the rotor is balanced and then rotate with it as one unit until the imbalance starts to change, or the disturbance of another origin emerges [14, 17–20].

The operability of ball auto-balancers at balancing the impellers of axial fans was studied experimentally in [21]. During the studies, there was no balancing of the impeller by correction mass, which did not make it possible to reveal the highest achievable quality of rotor balancing. The vibrating condition of the fans was examined based on the total vibrations, without determining the 1x vibration component. That reduced the assessment of quality of rotor balancing by ball auto-balancers.

Thus, it is a relevant task to investigate and compare the quality of balancing the impeller of an axial fan by correction mass with the quality of balancing the impeller by ball auto-balancers with the identification of 1x component of vibrations. This would make it possible to find out how accurately the ball auto-balancers balance the impeller, and to estimate whether it is expedient to apply ball auto-balancers for this purpose.

---

## 2. Literature review and problem statement

---

The general issue on reducing the noise and vibrations in axial fans has been addressed by many scientists [3–13]. It was shown in [3] that the main source of vibrations in axial fans is the typical imbalance of rotating parts in the assembly, as well as an aerodynamic imbalance. The latter arises from the inaccuracies in the manufacture of impellers, blades, due to the difference in gaps between the blades' crowns and a body, etc.

In high pressure fans, a gas (air) is compressible and therefore the imbalance should be referred to as gas-dynamic. In such fans, gas under high pressure passes through impellers, guiding devices, mazes of seals, etc. [4–7]. Therefore, the nature of the emergence of a gas-dynamic imbalance is complex, because it depends not only on the aerodynamic characteristics of blades, but also on the mechanism of their interaction with other parts of the fan. Patterns in the emergence of a gas-dynamic imbalance in turbo-assemblies in internal combustion engines are examined in [4], and paper [5] reported the calculation of this imbalance. Features and causes of the emergence of a gas-dynamic imbalance in gas-turbine engines were examined in [6]. It was established in [4–6] that the gas-dynamic imbalance significantly depends on the air density (temperature, height above sea level). It was determined in [4–6] that the gas-dynamic imbalance could also depend on the rotor speed, in particular due to the deformation of blades.

It is known that the best results in terms of vibration reduction could be provided by both the mass and aerodynamic balancing of an impeller. However, study [6] indicates that the aerodynamic imbalance (along with the mass one) of an aircraft GTE rotor can be balanced by correction mass. At the same time, balance would be disrupted when changing a flight's altitude, the engine's temperature, etc. It should be noted that the mass and aerodynamic disbalance of an impeller might be balanced purely aerodynamically (by changing the aerodynamics of individual blades). An interesting work in this regard is [8], whose authors investigated the effect exerted on the aerodynamic properties of a fan by through holes in the blade.

The aerodynamic, noise, and mass-inertial characteristics of a fan are influenced by the geometric shape of an impeller [9–12]. Therefore, separate tasks are to develop the structure of an impeller [9], to optimize the geometric parameters of blades in order to improve performance and reduce the mass of a fan [10], to perform the multi-criteria optimization of an impeller [11], to devise methods for optimizing the axial fan parameters [12], etc. However, the cited studies do not explore the mass and aerodynamic imbalance of an impeller.

In the production of axial fans, the blade rotor is consistently balanced aerodynamically and by correction mass prior to operation. An example is the technique described in [13]. Such a technology is time-consuming and, at present, it has no alternatives for high-pressure axial fans. The technology is applicable for low-pressure fans, but it does not make it possible to balance the variable imbalances during the operation of a fan.

Let us consider principal results that are applicable for balancing the impellers of low-pressure fans by passive auto-balancers.

Paper [14] examined a model in which a disc with blades (an impeller) was mounted on a flexible rotor and balanced by a two-ball auto-balancer. It was determined that at the speeds of rotor's rotation above resonance an auto-balancer balances the static components of both the mass and aerodynamic imbalance caused by the loss of a blade. The impeller is balanced on the move when using the technique described, but only statically.

Study [15] established an analogy between the mass and aerodynamic imbalances. The authors proved a possibility to balance them simultaneously by correction mass or with passive auto-balancers. It was found that the aerodynamic imbalance is directly proportional to the density of air and therefore varies depending on weather conditions and operational conditions for a fan.

Paper [16] determined the principal vector and the momentum of aerodynamic forces acting on a rotating impeller. The authors found the aerodynamic imbalance in the following cases: mounting an impeller on the rotor shaft with an eccentricity and skew; installing one blade at a different angle of attack; disruption of uniformity in the distribution of blades in a circle. It was established that the aerodynamic imbalance has a momentum component that is larger than static by an order of magnitude.

According to the results from studies [15, 16], the impeller of an axial fan should be balanced during operation, dynamically, by two passive auto-balancers. However, such a balancing has certain features. Let us consider them. When studying the process of auto-balancing, abstract models were theoretically explored in which a rotor carrying one [17] or two [18] auto-balancers rests on flexible supports. It was established [18] that it is possible to dynamically balance, with two passive auto-balancers, only a long rotor, and only at the speeds of rotation above resonance. However, the impeller itself is a short rotor and, therefore, it may seem that it is impossible to balance it by two passive auto-balancers.

Paper [19] described the type and structure of differential equations of motion and the balancing process of a rotary machine with auto-balancers. It was proven that a short rotor performs dynamically as the longer one provided the rotor is installed on rigid supports inside a heavy elastic-viscous enclosure. A conditionally longer rotor can be found, for example, in the differential equations of a system's movements, where part of the mass-inertial characteristics of the body is added to the mass-inertial characteristics of the rotor [20]. The impeller of an axial fan is actually installed on the rigid

supports inside an elastically-viscously fixed casing. That makes it possible to dynamically balance an impeller by two ball auto-balancers.

The process of the static and dynamic balancing of an impeller in the axial fan VO 06-300-4 by ball auto-balancers (with partitions) was experimentally investigated in [21]. It was found that the auto-balancers did not degrade the rotor's acceleration and rotation modes and reduce vibrations at a cruising speed of impeller rotation. It was established that the highest balance quality is ensured by two auto-balancers (dynamic balancing). The residual imbalance of an impeller was estimated at 10–15 % of the balancing capacity of auto-balancers.

The disadvantage of research undertaken in [21] is that the vibrations were not divided into 1x and non-1x. Therefore, in assessing a balance quality, the authors used total vibrations. This reduced the assessment of the balance quality of the impeller by auto-balancers. In addition, the authors did not balance the impeller by correction mass, which made it impossible to reveal the highest achievable balance quality of an impeller. Thus, it is a relevant task to address the flaws revealed.

### 3. The aim and objectives of the study

The aim of this study is to experimentally investigate and compare the balance quality of the impeller of an axial fan by correction mass and by ball auto-balancers.

That would make it possible to determine whether it is advisable to use ball auto-balancers for the automatic balancing of axial fans' impellers during operation.

To accomplish the aim, the following tasks have been set:

- to ensure high-quality manufacturing and mounting of auto-balancers on the shaft of an electric motor, to dynamically balance the rotating parts in the assembly, to determine the residual vibrations;

- to determine the natural (resonance) vibrations of a fan's casing installed at a bench and the first critical rotor rotation speed;

- to determine the residual vibrations when balancing, by two ball auto-balancers, rotating parts in the assembly in the absence and presence of imbalances in the two planes of correction.

### 4. Methods and equipment for experimental investigation of quality in balancing the impeller of an axial fan

#### 4.1. Configuration of the bench for balancing the impeller by correction mass and for evaluating the fan's vibration state

Fig. 1 shows the configuration of the mechanical part of the bench when balancing an impeller by correction mass and investigating the quality of balancing the impeller by ball auto-balancers.

When the impeller is balanced by correction mass, the auto-balancers have no balls. When investigating the quality of balancing an impeller by ball auto-balancers, balls are present in the auto-balancer.

Fig. 2 shows the configuration of the bench equipment when the impeller is balanced by correction mass and when checking the vibration state of the fan.

The vibration condition of a fan is characterized by the RMS of vibration speed, calculated by the device «Balkom-4» (Ltd «Kynematics», Russian Federation) based on the read-

outs from analog sensors of vibration accelerations 1–4. In this case, sensor 1 characterizes the operation of AB on the side of the impeller, 4 – on the fan's shank, 2 – radial beat on the casing between two AB, 3 – end side beat on the casing between two AB.

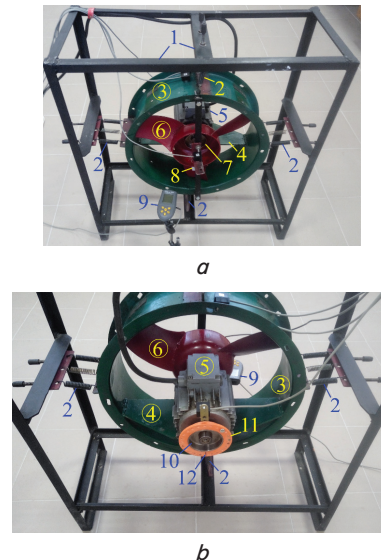


Fig. 1. Configuration of the mechanical part of the bench when balancing an impeller by correction mass and investigating the quality of balancing the impeller by ball auto-balancers: *a* – view from the side of an impeller; *b* – view from the side of a shank of an electric motor: 1 – frame; 2 – supports; 3 – protective casing (ring); 4 – shelf; 5 – electric motor; 6 – impeller; 7 – body of an auto-balancer from the side of an impeller; 8 – zero mark on the impeller; 9 – tachometer; 10 – auto-balancer's body on the shaft's shank; 11 – overlay for balancing; 12 – zero mark on the overlay

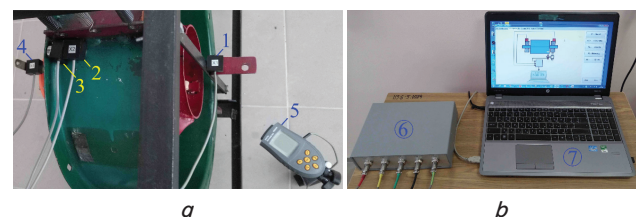


Fig. 2. Configuration of bench equipment at balancing an impeller by correction mass and checking the vibration state of a fan: *a* – arrangement of measuring equipment; *b* – measurement results processing equipment: 1 – sensor (of vibration accelerations) No. 1 – on the side of the impeller; 2 – sensor No. 2 – on the casing; 3 – sensor No. 3 – on the casing; 4 – sensor No. 4 – on the side of an electric motor's shank; 5 – tachometer; 6 – device «Balkom-4»; 7 – PC (laptop)

«Balkom-4» is a portable balancing kit. Designed to:

- measure the frequency of rotor rotation;
- measure, along 4 channels, RMS of the total and 1x component of a vibration speed (according to ISO Standard 10816 (ISO 10816-8:2014 «Mechanical vibration» – Evaluation of machine vibration by measurements on non-rotating parts – Part 8: Reciprocating compressor Systems», IDT) and ISO 2372 (ISO 20816-1:2016 Mechanical vibra-

tion – Measurement and evaluation of machine vibration – Part 1: General guidelines));

- balance a rotor in own supports in 1, 2, 3, 4 correction planes;
- conduct spectral analysis of vibrations based on vibration speeds.

The limits of absolute measurement error of the RMS of vibration speed, allowed at a base frequency (80 Hz) and in the operating frequency range, mm/s:  $\pm(0.1+0.1 \cdot V_m)$ , where  $V_m$  is the RMS of the measured vibration speed.

The device «Balkom-4» is used for:

- dynamic balancing of the rotating parts of a fan in the assembly;
- measuring the RMS of the total and 1x component of a vibration speed at 4 control points;
- spectral analysis of vibrations (based on vibration speeds).

#### 4. 2. Methods for determining the resonance and critical frequencies of rotor rotation, corresponding forms of oscillations and decrements of free damping oscillations

Note that the rotating parts of a fan in assembly are mounted on the rigid bearing supports inside an electric motor's body. The electric motor is rigidly mounted on a shelf that is rigidly connected to the protective casing of the fan. The protective casing is fixed in an elastic-viscous manner on flexible supports. Assume the elasticity-viscosity is described by the model of Kelvin-Voigt). At the working frequencies of impeller rotation, the movements of the protective casing are several orders of magnitude larger than the movements of rotating parts relative to the electric motor's casing.

Thus, the fan's casing is elastically fastened and has six degrees of freedom. Therefore, the casing has six resonance frequencies and six corresponding shapes of oscillations. In accordance with the general theory of rotary systems with auto-balancers, dynamic auto-balancing occurs at speeds exceeding the highest resonance rotation speed of the rotor [19]. Therefore, these speeds are needed to check whether the rotor rotates at the required angular velocity.

For auto-balancing to occur, viscous friction is required. Therefore, it is necessary, for each shape of free oscillations corresponding to the resonance frequencies, to find a logarithmic decrement of damping.

The fan should work at a distance from critical frequencies – at which there are significant oscillations of the frame, fan blades, etc. Therefore, it is necessary to find the lowest critical rotation speed of the impeller for a given bench.

To excite mechanical oscillations of the bench, we apply the designed controlled generator of mechanical oscillations (Fig. 3).

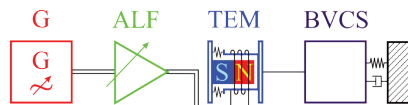


Fig. 3. Enlarged block diagram of the controlled mechanical oscillations generator

In Fig. 3, the following designations are used:

- G – generator of free- and standard-shaped signals (JDS2900, PRC: 0–15 MHz, used to generate the sinusoidal signals with a frequency from 0 to 100 Hz with a step of 0.01 Hz and amplitude from 1 to 20 V with a step of 1 V);

- ALF – low frequency amplifier (JVC KS-AX202, Japan: frequency range is 5–50,000 Hz (–3 dB), used to amplify the generator's signal);

- TEM – linear electromechanical transducer (vibrational speaker, PRC: 25 W, 4 Ohms, 0–20,000 Hz, used to excite a sinusoidal disturbing force of variable amplitude and frequency from 0 to 100 Hz);

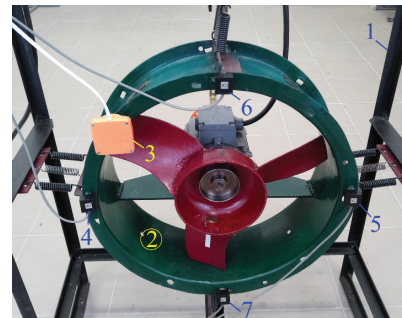
- BVEF – visco-elastic fixed body (a casing of the axial fan).

Mechanical oscillations of the bench are examined based on readouts from four sensors-accelerometers  $\pm 3g$  (from the device «Balkom-4»). The sensors are mounted on the protective casing or the frame of the bench, depending on the examined oscillation shape. Analog signals from the sensors are processed by the modified device oscilloscope motor-tester MT Pro 4 (MLab, Ukraine). In particular, the device can:

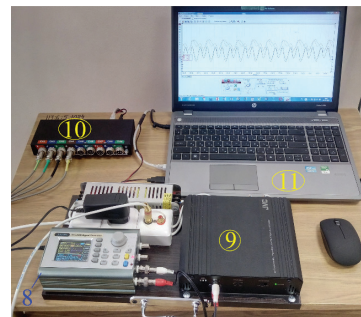
- digitize signals along 8 analog channels;
- work with a single logical channel;
- operate under the modes of an oscilloscope, recorder, spectrum analyzer.

Modernization implies the installation, into the device, of sources of stabilized power, 3.3 V, replacing connectors of the type BNC on the GX16 type connectors. The modernization makes it possible to connect directly to the oscilloscope the sensors of vibration accelerations from the device «Balkom-4».

Configuration of the mechanical part of the bench and equipment in determining the resonance and critical frequencies, as well as the corresponding shapes of oscillations, is shown in Fig. 4.



a



b

Fig. 4. Configuration of the bench for determining the natural (resonance) frequencies and shapes of oscillations by the fan's casing, as well as critical frequencies and the corresponding shapes of oscillations by the bench:

- a – mechanical part; b – equipment; 1 – frame;
- 2 – fan's casing; 3 – linear electromechanical transducer (the oscillation axis is parallel to the rotor's longitudinal axis); 4 – sensor No. 1; 5 – sensor No. 2; 6 – sensor No. 3;
- 7 – sensor No. 4; 8 – signal generator; 9 – low frequency amplifier; 10 – digital USB oscilloscope; 11 – laptop

The natural oscillation frequencies (resonance frequencies) and the first critical frequency of the bench oscillations were determined by the following procedure. An electromechanical converter is attached to the fan’s casing in such a way as to maximally create a certain shape of resonance oscillations. Four sensors of vibration accelerations are placed on the casing so that they most effectively register the corresponding shape of resonance oscillations. The signal generator creates the sinusoidal signals; they are amplified by the amplifier of low frequency and sent to the electromechanical transducer. Changing the oscillation frequency by the generator establishes the frequency range at which there occur the most intense oscillations of the casing in the corresponding shape. The oscillation shape was tested by signals from the sensors of accelerations (digitized by a USB oscilloscope). The resonance (critical) frequency  $n$  is the middle of the found range. To assess the width of the range, we specify the average value of  $n$  and  $\pm\Delta n/2$ , where  $\Delta n$  is the width of the found range.

*Procedure for determining the logarithmic decrement of damping of different-shaped oscillations.* The electromechanical converter creates the most intense oscillations of a certain resonance or critical shape. The USB oscilloscope is set into a self-recorder mode to record a signal from the sensor that fluctuates most intensively. The electromechanical transducer is deactivated. A signal from the sensor is recorded until oscillations fade. The signal is saved as a table in the Excel format. The truncated table is processed in a software package for statistical analysis («Statistica»). It is assumed that vibration accelerations change in line with the following law:

$$a(t) = Ae^{-\beta t} \sin(2\pi n t + \varphi_0), \tag{1}$$

where  $A$  is amplitude;  $\beta$  is the coefficient of viscous resistance forces,  $n$  is the resonance (or critical) frequency,  $\varphi_0$  is the initial phase. Coefficients  $A, \beta, n, \varphi_0$  are determined from the truncated table by a least square method.

Then the frequency, period, logarithmic decrement of damping free oscillations at a resonance frequency, are, respectively, equal to:

$$n, T = 1/(2\pi n), \lambda = \beta T = \beta / (2\pi n). \tag{2}$$

It should be noted that:

- 1) coefficients  $A, \varphi_0$  depend significantly on the sample data while coefficients  $n, \beta$  are almost independent;
- 2) coefficients  $n, \beta$  are determined less stable if we represent, in law (1), an amplitude  $A$  in the form (considering  $a(t)$  to be acceleration):

$$A = A_0 (2\pi n)^2. \tag{3}$$

Small magnitudes of vibration accelerations reduce the accuracy of calculations. Therefore, the logarithmic decrements of oscillations damping are rounded up to the nearest number in increments of 0.005.

**4. 3. Parameters for auto-balancers and a procedure for checking their operability**

Ball auto-balancers have a treadmill, a lid with a hole for pouring oil, a bolt to fix the lid, and balls. The lid closes the ring hole hermetically, allowing it to fill it with oil.

The balancing capacity of an auto-balancer was determined from formula [22]:

$$S(n) = \frac{m(R-r)^2}{r} \sin\left(n \cdot \arcsin \frac{r}{R-r}\right), \tag{4}$$

where  $n$  is the number of balls,  $m$  is the mass,  $r$  is the ball’s radius,  $R$  is the treadmill’s radius.

In the experiments, we used six-ball AB ( $n=6$ ) with balls of diameter  $d = 2r = 11.9$  mm and mass  $m = 6.93$  g. In this case, an AB has in the impeller plane the diameter of a treadmill of  $D_{im} = 2R_{im} = 68$  mm and a balancing capacity  $S_{im}^{(AB)} = 878.57$  g·mm, and in the plane of the shank –  $D_{sh} = 2R_{sh} = 64$  mm and  $S_{sh}^{(AB)} = 776.42$  g·mm.

To verify the advent of auto-balancing, we check the arrangement of balls in an auto-balancer regarding the imbalance. To this end, we exploit a camera with the flash [21].

**5. Results of experimental study into the quality of static and dynamic balancing**

**5 1. Ensuring high-quality manufacturing and installation of auto-balancers on the electric motor shaft, balancing of rotating parts by correction mass**

*Minimizing treadmill beats.* After installing auto-balancers on the electric motor’s shaft, the electric motor with rotating parts in assembly was mounted on a lathe. As described in [21], by using the lathe feed and natural rotation of the fan’s electric motor, we smoothed the treadmills. After that, we tested the achieved radial and side treadmill beats. Measurements were carried out by clock type indicators (with a lever to measure radial beats) whose measuring scale was divided into 0.01 mm. For the auto-balancer, both on the side of the impeller and from the side of the shank the radial and side beats were 0.00 mm. That should ensure quality operation of auto-balancers.

*Balancing the rotating parts of a fan by correction mass.* Results from measuring the RMS of vibration speed by sensors before and after balancing are given in Table 1.

Table 1

Vibration state of the fan before and after two-plane balancing

Magnitude, measuring unit	Sensors readouts							
	Before balancing				After balancing			
	1	2	3	4	1	2	3	4
$ V_j^{(gen)} $ , mm/s	4.21	2.09	5.08	3.19	1.31	1.40	1.13	1.46
$ V_j^{(rev)} $ , mm/s	3.65	1.48	4.40	1.89	0.119	0.175	0.184	0.106
$\varphi_j$ , degree	286.6	240.7	132.3	154.4	218.5	186.1	158.2	171.2

Table 1 gives the average values of magnitudes based on the results from 5 measurements. Deviations from the average values are caused by accuracy of measurements, provided by the device «Balkom-4», and do not exceed 0.01 mm/s.

As regards balancing, the main components of vibration speeds are 1x, that is, those that can be reduced in balancing. Table 2 gives the results from splitting the 1x component of RMS of vibration speed into the static and momentum ones.

Table 2

Static and momentum components of 1x components of RMS of vibration speed, measured before balancing

Sensor	1		2	4	
	static	momentum	1x	static	momentum
Magnitude, mm/s	1.38	2.56	1.48	1.38	2.56
Phase, degree	256.1	302.5	240.7	256.1	122.5

Table 2 shows that the residual vibrations have:

- a static component, which is close to readouts from sensor 2;
- a momentum component whose phase is close to sensor 3 readings.

This confirms the assumption that sensor 2 responds better to the static component of vibration speeds, and sensor 3 to the momentum one.

A large momentum component of RMS of vibration speed is due to that the rotating parts of a fan are balanced at a plant-manufacturer statically, in the impeller plane.

Fig. 5 shows spectral diagrams that were built based on vibration speeds before (Fig. 5, a) and after (Fig. 5, b) balancing of rotating parts in assembly.

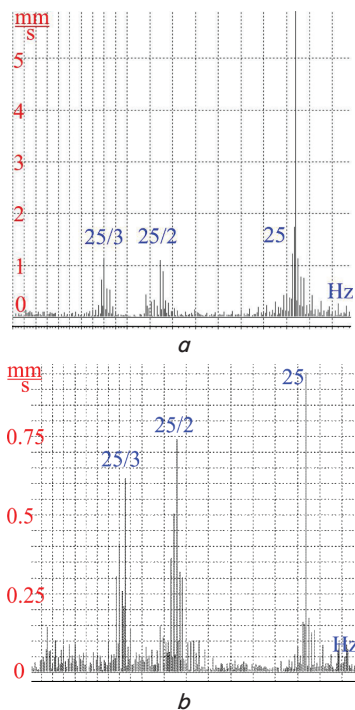


Fig. 5. Spectral diagram constructed based on vibration speeds: a – before balancing, b – after

Table 1 and Fig. 5, a show that before balancing the vibrations mostly occur at the frequency of impeller rotation (25 Hz) and are the 1x vibration component. Non-1x vibration components are insignificant and occur at subfrequencies of 25/2 and 25/3.

Table 1 and Fig. 5, b demonstrate that, after balancing, the main vibrations occur at subfrequencies of 25/2 and 25/3 and are the non-1x. The 1x components (at the frequency of impeller rotation of 25 Hz) are almost an order of magnitude less. By correction mass, the 1x component of RMS of

vibration speed are reduced, from the side of an impeller, by 30 times, from the side of a shank – by 18 times.

The emergence of subharmonic vibrations is difficult to clearly explain at this stage of our study.

Initial unbalances when the impeller is balanced by correction mass are:

$$S_{im0} = 1.1 \times 74 = 81.4 \text{ g} \cdot \text{mm};$$

$$S_{sh0} = 2.4 \times 48 = 115.2 \text{ g} \cdot \text{mm},$$

where 1.1 g is the corrective mass from the side of an impeller, 74 mm is the radius of setting this mass, 2.4 g is the corrective mass from the side of an impeller, 48 mm is the radius of setting this mass.

Residual imbalances when balancing the impeller by correction mass are:

$$\Delta S_{im} = 7.4 \text{ g} \cdot \text{mm};$$

$$\Delta S_{sh} = 7.2 \text{ g} \cdot \text{mm}.$$

Attempts to improve the vibration state of a fan by corrective loads with masses smaller than 0.1 g in a fairing and 0.15 g in a shank have been futile.

### 5.2. Determining the natural oscillation frequencies (resonance frequencies) and the first critical oscillation frequency

The principal shapes of resonance oscillations and the first shape of critical oscillations are shown in Fig. 6.

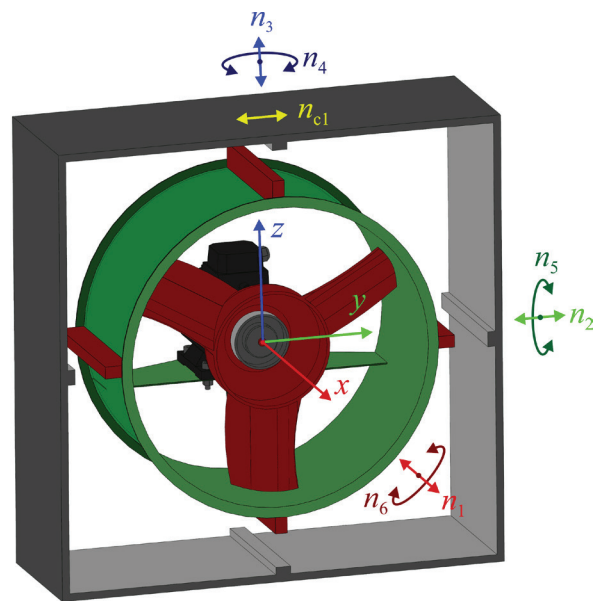


Fig. 6. Principal frequencies and shapes of resonance oscillations by the fan's casing, and the first frequency and shape of critical oscillations by the bench

Fig. 7 shows a fragment of the oscillogram of vibration accelerations at the rotating oscillations of the casing around the y axis.

The oscillogram shows that sensors 1 and 2 are almost motionless (are along the y axis), and sensors 3 and 4 fluctuate in the counterphase. At resonance, all other harmonics

disappear and there remain pure harmonic oscillations at frequency  $n_5$ . The oscillogram can be used to roughly find a resonance frequency:

$$n_5 \approx 1 / (195.596 - 195.517) = 12.66 \text{ Hz.}$$

However, it is determined more accurately based on readouts from a pulse generator.

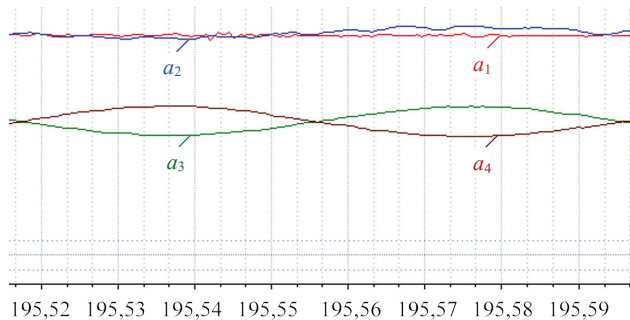


Fig. 7. A fragment of the oscillogram of vibration speeds at the rotating oscillations of the casing around the  $y$  axis at frequency  $n_5$

Table 3 gives the magnitudes of resonance and critical frequencies, logarithmic decrements of oscillations damping.

Table 3

Magnitudes of resonance and critical frequencies, logarithmic decrements of oscillations damping

No.	Description of oscillation shape	Frequency, Hz	Logarithmic decrement
Resonance oscillations of fan's casing			
1	Translational along the $x$ axis	$n_1 = 5.72 \pm 0.04$	0.01
2	Close to translational along the $y$ axis	$n_2 = 7.88 \pm 0.02$	0.015
3	Close to translational along the $z$ axis	$n_3 = 8.14 \pm 0.02$	0.015
4	Rotations around the $z$ axis	$n_4 = 12.09 \pm 0.03$	0.015
5	Rotations around the $y$ axis	$n_5 = 12.72 \pm 0.03$	0.015
6	Rotations around the $x$ axis	$n_6 = 15.39 \pm 0.04$	0.01
Critical frequencies and shapes of bench oscillations			
1	Skew frame deformation	$n_{c1} = 32.74 \pm 0.03$	0.01

Table 3 shows the fan operates at a rotation speed above resonance at a distance from the largest resonance frequency and at a pre-critical frequency at a distance from the 1st critical frequency.

Thus, the conditions for fixing the fan's casing should contribute to the occurrence of auto-balancing.

At this stage of research, it is already possible to explain the emergence of residual vibrations at subharmonic frequencies. The subharmonic frequency  $25/2$  is close to resonance frequencies  $n_4, n_5$ . The subharmonic frequency  $25/3$  is close to resonance frequencies  $n_2, n_3$ . Thus, the non-1x (subharmonic) oscillations are caused by the impeller rotating at a frequency that is 3 times larger than resonance frequencies  $n_4, n_5$ , and is twice as large as resonance frequencies  $n_2, n_3$ .

At the current stage of research, it can be argued that the 1x component of vibrations, given in Table 3, measured after balancing, are the magnitudes, which can be ensured by auto-balancers at perfect operation. The non-1x vibration components can vary significantly depending on patterns of fixing a fan's casing and other factors.

### 5. 3. Determining residual vibrations when a fan is balanced by two ball auto-balancers

#### 5. 3. 1. Residual vibrations when installing balls in auto-balancers into the balanced fan

With balls in an AB, the stability of readouts from the device «Balkom-4» is reduced to 0.015 mm/s, provided that the auto-balancing has occurred and the fan is not restarted. Restarting the fan renders unstable all the device's readings. The most unstable are the 1x component of RMS of vibration speed and the corresponding phase angles. However, the 1x component of RMS of vibration speed from sensors No. 1 and No. 4 have an upper limit of magnitude 0.3 mm/s. Total components of RMS of vibration speed from sensors No. 1 and No. 4 have an upper limit of magnitude 2.00 mm/s.

Thus, balls in an AB can increase the 1x component of RMS of vibration speed by almost 3 times, and the magnitude of a 1x component does not exceed 0.3 mm/s. The total RMS of vibration speed also increases, but does not exceed 2.00 mm/s.

#### 5. 3. 2. Residual vibrations in the presence of imbalance in two planes of correction

1. *Creating a dynamic imbalance.* We put a load to a fairing at the zero level, a mass of 6.2 g, at a distance of 74 mm from the longitudinal axis. On the side of the shank, on a balancing disk, at the level of  $90^\circ$ , the second unbalanced load was installed, weighing 5.7 g. The unbalanced masses create, respectively, the following imbalances in the planes of auto-balancers from the side of an impeller and shank:

$$S_{im} = 6.2 \times 74 = 458.8 \text{ g} \cdot \text{mm}, \angle 0^\circ;$$

$$S_{sh} = 5.7 \times 48 = 273.6 \text{ g} \cdot \text{mm}, \angle 90^\circ.$$

2. *Determining a vibration state.* The results from determining a vibration state of the fan without balls and with the balls in auto-balancers are given in Table 4.

Table 4

Vibrational state of a fan with and without balls in AB

Magnitude, measuring unit	Sensors readouts							
	Before balancing				After balancing			
	1	2	3	4	1	2	3	4
$ V_j^{(gen)} , \text{ mm/s}$	8.43	4.98	6.47	6.06	<2.00	<2.00	<2.00	<2.00
$ V_j^{(rec)} , \text{ mm/s}$	8.32	4.81	6.28	5.81	<0.3	<0.3	<0.3	<0.3
$\phi_j, \text{ degree}$	13.9	36.1	172.1	116.2	-	-	-	-

3. *Explanation of instability in the readings from the device «Balkom-4».* By taking photographs with the flash (Fig. 8), it was checked that the balls in auto-balancers, both in a fairing (Fig. 8, a) and on a shank (Fig. 8, b) entered the autobalancing position. Re-photographing after a certain time made it possible to check that the balls stopped moving relative

the auto-balancers' casings. Re-starting and photographing helped us check that the balls eventually enter the autobalancing position. These positions do not change with starting and restarting a fan. The balls do not visually change their positions after the setting of autobalancing.

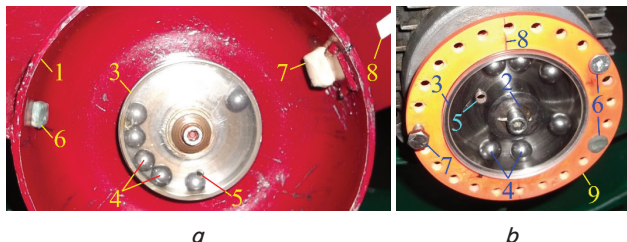


Fig. 8. Checking auto-balancers operation by photographing with the flash: *a* – in a fairing; *b* – on a shank; 1 – fairing; 2 – electric motor's shank; 3 – auto-balancer's casing; 4 – balls; 5 – hole in the lid of the auto-balancer to add lubricants; 6 – corrective loads, with which the rotating parts were balanced; 7 – a load creating an imbalance; 8 – zero mark (from which we counted angles in the direction of impeller rotation); 9 – auto-balancer's nozzle for balancing

Thus, the instability in readings from the device «Balkom-4» is explained by the fact that after each restart of a fan the balls enter a new auto-balancing position.

Therefore, regardless of the magnitudes of imbalances in two planes, two auto-balancer balance the rotating parts in assembly with the same quality.

## 6. Discussion of results on investigating the quality of balancing an axial fan by correction mass and by passive auto-balancers

The main source of vibrations in axial fans after a manufacturer is the dynamic residual imbalance of an impeller. The principal component of vibration speeds is 1x (a frequency of 25 Hz), that is the one that can be reduced by balancing. The non-1x vibration components occur at subharmonic frequencies 25/2 and 25/3 and are smaller by an order of magnitude.

When the impeller is balanced by correction mass the initial imbalances are  $S_{im0} = 81.4 \text{ g}\cdot\text{mm}$ ,  $S_{sh0} = 115.2 \text{ g}\cdot\text{mm}$ , and residual –  $\Delta S_{im} = 7.4 \text{ g}\cdot\text{mm}$ ,  $\Delta S_{sh} = 7.2 \text{ g}\cdot\text{mm}$ .

After balancing the impeller by correction mass the main contribution to the residual vibrations is made by the non-1x vibration components occurring at subharmonic frequencies 25/2 and 25/3. The contribution to the residual vibrations of the subharmonic components is almost an order of magnitude greater than the contribution of 1x vibration component.

The result obtained agrees with the fact that impellers are balanced statically and in the impeller plane by a manufacturer.

A protective casing, flexibly mounted on a frame, has 6 resonance oscillation frequencies, the smallest of which is  $n_1 = 5.72 \pm 0.04 \text{ Hz}$ , and the largest is  $n_6 = 15.39 \pm 0.04 \text{ Hz}$ . The first critical speed of impeller rotation for the bench is  $n_{c1} = 32.74 \pm 0.03 \text{ Hz}$ . At this frequency there occur considerable deformations of the frame in terms of skew. The impeller rotates at a speed above resonance but at subcritical frequency at a distance from resonances.

Logarithmic decrements of free oscillations damping at a resonance or critical frequency are not less than 0.01. The

resonance frequencies  $n_2$  and  $n_3$  (almost translational oscillations of the casing along the axes  $y$  and  $z$ , respectively) are close to the subharmonic frequency 25/3. The resonance frequencies  $n_5$  and  $n_6$  (turnover oscillations of the casing around the axes  $z$  and  $y$ , respectively) are close to the subharmonic frequency 25/2. Closeness of resonance frequencies to subharmonic explains the presence of non-1x residual vibrations at subharmonic frequencies.

Thus, the non-1x vibration components of residual vibration are significantly dependent on fixing a fan's casing (resonance and critical frequencies). Therefore, it is not possible to estimate the quality of rotor balancing by passive auto-balancers based on these components.

Following the balancing of an impeller by auto-balancers, the main contribution to the residual vibrations is made by the non-1x vibration components occurring at subharmonic frequencies 25/2 and 25/3. The contribution to the residual vibrations of the subharmonic components is almost 5 times larger than the contribution of 1x vibration component.

Balancing capacities of auto-balancers on the side of an impeller and a shank, are, respectively,  $S_{im}^{(AB)} = 878.57 \text{ g}\cdot\text{mm}$ ,  $S_{sh}^{(AB)} = 776.42 \text{ g}\cdot\text{mm}$ .

The residual imbalances when the impeller is balanced by ball auto-balancers are:

$$\delta S_{im} < 3\Delta S_{im} = 22.2 \text{ g}\cdot\text{mm};$$

$$\delta S_{sh} < 3\Delta S_{sh} = 21.6 \text{ g}\cdot\text{mm}.$$

Consequently, auto-balancers respond to imbalances, constituting not less than 3% of their balancing capacity. This is the sensitivity of auto-balancers to imbalance. Previously [20], the sensitivity was considered to be worse (10–15%). Understatement [21] of balancing quality (and the sensitivity of auto-balancers to imbalance) was due to that the quality was estimated based on the total, rather than non-1x components of RMS of vibration speed.

Correction mass can accurately balance an impeller, but the achieved quality of balancing will not last long.

The results were obtained for a specific bench built for the fan VO 06-300-4. Therefore, the results are of partial character. However, these results may be applicable for fans of the series VO 06-300/VO-12-300 series; VOG/VO-15-320; VO 2,3-130/VO 46-130 due to the similarity of fan designs.

The results of our research prove the possibility of dynamic balancing by two ball auto-balancers of a short rotor, provided that the rotor is mounted on rigid supports inside a massive casing, while the body is visco-elastically fixed. This can be used in the development of auto-balancers for balancing similar rotors – drums in washing machines with frontal loading, extractors in juicers, etc.

In the future, it is planned to experimentally investigate the aerodynamic disbalance of the impeller of a low type axial fan and it's balancing by correction mass.

## 7. Conclusions

1. An axial fan after manufacturing has the RMS of vibration speed on the casing of the fan, which, with a margin, correspond to the balance quality grade: 1x – G2.5; total – G6.3. The main source of vibrations in axial fans is the dynamic residual imbalance of the impeller. The principal component of the vibration speed is 1x (a frequency of 25 Hz), that is the



one that can be reduced by balancing. The non-1x vibration components occur at subharmonic frequencies 25/2 and 25/3 and are smaller by an order of magnitude.

When an impeller is balanced by correction mass, the initial imbalances on the side of an impeller and a shank are, respectively, 81.4 and 115.2 g·mm, and the residual – 7.4 and 7.2 g·mm. The magnitudes of RMS of vibration speed can be reduced on the fan's casing to magnitudes corresponding to the following balance quality grade (with a margin): 1x – G0.4; total – G2.5. The main contribution to the residual vibrations is made by the non-1x vibration components occurring at subharmonic frequencies. The contribution to the residual vibrations of the subharmonic components is almost an order of magnitude greater than the contribution of 1x vibration component.

2. A protective casing, flexibly mounted on the frame, has 6 resonance oscillation frequencies, the largest of which is 1.6 times less than the speed of impeller rotation. The first critical speed of impeller rotation is 1.3 times larger than the working frequency of impeller rotation. At the first critical frequency there occur large deformations of the frame in terms of skew. Thus, the impeller rotates at a frequency above the resonance but subcritical at a distance from resonances and critical frequencies.

Logarithmic decrements of free oscillations damping with resonance or critical frequency are not less than 0.01.

The resonance frequencies  $n_2$  and  $n_3$  (almost translational oscillations of the casing along the axes  $y$  and  $Z$ , respectively) are close to the subharmonic frequency 25/3. The resonance frequencies  $n_5$  and  $n_6$  (rotational oscillations of the casing fluctuations around the axes  $z$  and  $y$ , respectively) are close to the subharmonic frequency 25/2. Closeness of the resonance frequencies to subharmonic explains the presence of non-1x residual vibrations at subharmonic frequencies.

3. The dynamic balancing of an impeller by two ball auto-balancers can reduce the RMS of vibration speed on the fan's casing to the magnitudes corresponding to the following class of balancing quality: 1x – G0.4; total – G2.5.

After balancing an impeller by correction mass, the main contribution to the residual vibrations is made by the non-1x vibration components occurring at subharmonic frequencies 25/2 and 25/3. The contribution to the residual vibrations of the subharmonic components is almost 5 times larger than the contribution of 1x vibration component.

Balancing capacities of auto-balancers on the side of an impeller and a shank are, respectively, 878.57 and 776.42 g·mm. The residual imbalances when an impeller is balanced by ball auto-balancers from the side of an impeller and a shank are, respectively, 22.2 and 21.6 g·mm. Auto-balancers responds to imbalances, constituting not less than 3 % of their balancing capacity.

## References

1. Polyakov, V. V., Skvortsov, L. S. (1990). *Nasosy i ventilyatory*. Moscow: Stroyizdat, 336.
2. Ventilyatory osevye. Available at: <http://gradvent.org.ua/ventilyatory/ventilyatory-osevye>
3. Ziborov, K. A., Vanzha, G. K., Mar'enko, V. N. (2013). Disbalans kak odin iz osnovnyh faktorov vliyayushchih na rabotu rotorov shahtnyh ventilyatorov glavnogo provetrivaniya. *Sovremennoe mashinostroenie. Nauka i obrazovanie*, 3, 734–740.
4. Korneev, N. V. (2008). Aerodinamicheskiy disbalans turboagregatov i algoritmy ego prognozirovaniya. *Mashinostroitel'*, 10, 24–27.
5. Korneev, N. V., Polyakova, E. V. (2014). Raschet aerodinamicheskogo disbalansa rotora turbokompressora DVS. *Avtomobil'naya promyshlennost'*, 8, 13–16.
6. Idel'son, A. M. (2003). Modelirovanie aerodinamicheskogo disbalansa na lopatkah ventilyatora. *Problemy i perspektivy razvitiya dvigatelestroeniya: trudy MNTK. Samar. gos. aerokosm. un-t im. S. P. Koroleva. Ch. 2. Samara: SGAU*, 180–185.
7. Idelson, A. M., Kuptsov, A. I. (2006). Elastic deformation of fan blades as a factor, influencing the gas-dynamic unbalance. *Vestnik SGAU*, 2-1 (10), 234–238.
8. Yang, X., Wu, C., Wen, H., Zhang, L. (2017). Numerical simulation and experimental research on the aerodynamic performance of large marine axial flow fan with a perforated blade. *Journal of Low Frequency Noise, Vibration and Active Control*, 37 (3), 410–421. doi: <https://doi.org/10.1177/0263092317714697>
9. Almazo, D., Rodríguez, C., Toledo, M. (2013). Selection and Design of an Axial Flow Fan. *World Academy of Science, Engineering and Technology International Journal of Aerospace and Mechanical Engineering*, 7 (5), 923–926.
10. Liu, Z., Han, B., Yeming, L., Yeming, L. (2017). Application of the objective optimization algorithm in parametric design of impeller blade. *Journal of Tianjin University (Science and Technology)*, 50 (1), 19–27. doi: <http://doi.org/10.11784/tdxbz201508001>
11. Qu, X., Han, X., Bi, R., Tan, Y. (2015). Multi-objective genetic optimization of impeller of rail axial fan based on kriging model. *Zhongguo Jixie Gongcheng/China Mechanical Engineering*, 26 (14), 1938–1943. doi: <http://doi.org/10.3969/j.issn.1004-132X.2015.14.017>
12. Bamberger, K., Carolus, T. (2017). Development, Application, and Validation of a Quick Optimization Method for the Class of Axial Fans. *Journal of Turbomachinery*, 139 (11). doi: <https://doi.org/10.1115/1.4036764>
13. Suvorov, L. M. (2009). Pat. No. 2419773 RU. Sposob nizkooborotnoy balansirovki massy i aerodinamiki vysokooborotnogo lopatochnogo rotora. MPK G01M 1/00 (2006.01). No. 2009109011/28; declared: 11.03.2009; published: 27.05.2011, Bul. No. 15.
14. DeSmidt, H. A. (2010). Automatic Balancing of Bladed-Disk/Shaft System via Passive Autobalancer Devices. *AIAA Journal*, 48 (2), 372–386. doi: <https://doi.org/10.2514/1.43832>
15. Filimonikhin, G., Olijnichenk, L. (2015). Investigation of the possibility of balancing aerodynamic imbalance of the impeller of the axial fan by correction of masses. *Eastern-European Journal of Enterprise Technologies*, 5 (7 (77)), 30–35. doi: <https://doi.org/10.15587/1729-4061.2015.51195>

16. Olijnichenko, L., Filimonikhin, G., Nevdakha, A., Pirogov, V. (2018). Patterns in change and balancing of aerodynamic imbalance of the lowpressure axial fan impeller. *Eastern-European Journal of Enterprise Technologies*, 3 (7 (93)), 71–81. doi: <https://doi.org/10.15587/1729-4061.2018.133105>
17. Ryzhik, B. Sperling, L. Duckstein, H. (2004). Auto-Balancing of Anisotropically Supported Rigid Rotors. *Technische Mechanik*, 24 (1), 37–50. Available at: [http://www.uni-magdeburg.de/ifme/zeitschrift\\_tm/2004\\_Heft1/ryzhik\\_autobalancing.pdf](http://www.uni-magdeburg.de/ifme/zeitschrift_tm/2004_Heft1/ryzhik_autobalancing.pdf)
18. Rodrigues, D. J., Champneys, A. R., Friswell, M. I., Wilson, R. E. (2008). Automatic two-plane balancing for rigid rotors. *International Journal of Non-Linear Mechanics*, 43 (6), 527–541. doi: <https://doi.org/10.1016/j.ijnonlinmec.2008.01.002>
19. Goncharov, V. V., Filimonikhin, G. B. (2015). Form and structure of differential equations of motion and process of auto-balancing in the rotor machine with auto-balancers. *Izvestiya Tomskogo politehnicheskogo universiteta. Inzhiniring georesursov*, 326 (12), 20–30. Available at: [http://www.lib.tpu.ru/fulltext/v/Bulletin\\_TPU/2015/v326/i12/02.pdf](http://www.lib.tpu.ru/fulltext/v/Bulletin_TPU/2015/v326/i12/02.pdf)
20. Artyunin, A. I., Eliseev, S. V., Sumenkov, O. Y. (2018). Determination of parameters and stability zones of pendulum auto-balancer of rotor, installed in housing on elastic supports. *Proceedings of the International Conference «Aviamechanical Engineering and Transport» (AVENT 2018)*. doi: <https://doi.org/10.2991/avent-18.2018.5>
21. Olijnichenko, L., Goncharov, V., Sidei, V., Horpynchenko, O. (2017). Experimental study of the process of the static and dynamic balancing of the axial fan impeller by ball auto-balancers. *Eastern-European Journal of Enterprise Technologies*, 2 (1 (86)), 42–50. doi: <https://doi.org/10.15587/1729-4061.2017.96374>
22. Goncharov, V., Filimonikhin, G., Nevdakha, A., Pirogov, V. (2017). An increase of the balancing capacity of ball or roller-type auto-balancers with reduction of time of achieving auto-balancing. *Eastern-European Journal of Enterprise Technologies*, 1 (7 (85)), 15–24. doi: <https://doi.org/10.15587/1729-4061.2017.92834>